THE FOLLOWING MANUSCRIPT IS A CORRECTED VERSION OF THE JOURNAL PUBLICATION "IEEE TRANSACTIONS ON PLASMA SCIENCE, DECEMBER 2017".

Koehler, D. Radiation-Absorption and Geometric-Distortion and Physical-Structure Modeling. *IEEE Transactions on Plasma Science*. **45**, 3306 (2017).

Radiation absorption, geometric-distortions and physical structure modeling

D.R. Koehler
Sandia National Laboratories (retired) , 87185, USA

Abstract. As latter-day experimental interstellar and intergalactic astronomical data are being related to unknown forms of cosmological energies (hypothesized as dark-energy and dark-matter), we, in the present development, attribute radiation-absorption properties to the universe's electromagnetic energy content or to the universe's geometric manifold itself. Therefore, for either an electromagnetic energy content or a manifold-energy content (manifold-curvature with radiation absorption), we advance a classical optical attenuation-coefficient model to describe energy propagation throughout the universe thereby providing an alternative analysis and cosmological explanation for the experimental radiative-astronomical data. This modeling is applicable whether one attributes radiation-attenuation to the presence of additional universe-bearing electromagnetic energy sources or as an interpretation of the geometric manifold as a substantive and locally distortable entity. For the geometric-manifold absorption description, the spacetime-absorption-property concept is further utilized to model a radiatively decaying blackbody as the genesis of a propagating decaying shock-wave, which in turn is posited as the energy source to mimic a spatially-distorted universe. The earlier derived composite coupling-constant (gravitational and electromagnetic) is inherently incorporated to classify the elements of the seeded universe. Energy densities derived from a distorted-spacetime model are further assimilated in a fundamental manner to describe the ensuing features of the explosive blackbody event.

Keywords— Astronomy, Cosmology, General Relativity, Geometry, Plasmas, Structural stability

1. Introduction

We consider electromagnetic-energy components as fundamental components in inter-stellar and inter-galactic "space"; this consideration results in modeling with an absorption-dependent (μ) radiation propagation energy, $h\nu(\mu)$. The presence of electrically- and/or magnetically-active species throughout any propagating medium would produce an observable and acknowledged impact on the propagating radiation energy [1-9] and alternatively explain propagated radiation energy (frequency) shifts throughout the universe thereby impacting distance, size and age characterizations.

Similarly, a substantive or absorptive transmission-medium model for the spacetime manifold geometry itself would also generate a different explanation and analysis of experimental astronomical data; these models are developed in the "Radiation Propagation in the Manifold" section to follow.

In the "Distortional Energy Decay" section, the spacetime-absorption-property concept is further utilized to model a radiatively decaying blackbody as the genesis of a propagating decaying shock-wave, which in turn is posited as the energy source to mimic a locally spatially-distorted universe. For this distorted geometry modeling, we maintain and expand the geometrical perspectives inherent in a "Curved empty space as the building material of the physical world" supposition [10-15]. Building on the earlier work [14,15], we apply the geometric concepts to a distortional-geometric entity, a local-universe mimic, modeled as an unstable radiating blackbody, producing to extinction a spherically propagating and decaying "shock-wave" (the present terminology to describe the approximate "rectangular(time) emission function", see Figure 7) in the geometric-manifold. The shock-wave decays by virtue of the posited absorption-characteristic for the spacetime manifold. In the earlier work the classical Riemannian four-dimensional geometrical curvature equations were applied to describe localized distortional-energy-distributions, with a modified-gravitational model-derived coupling-constant between geometry and physical energy, and making no distinction between "ordinary matter and dark matter" [14,15].

The "negative energy-density" spatial regions manifested in the earlier "distorted fundamental-particle mimics"

are not suggested in the large-magnitude energy-density model here employed, however the "geometric maximum-energy-density" feature (successfully exploited to geometrically explain and quantify the Fermi constant [14]) is included, as well as the distortional-electron feature.

In the case of the distorted-geometry model, although no localized distortional metric is here constructed, the infinitesimal nature of the absorption coefficient μ does not materially change the calculational procedure or results. However see the work of [16-20] where cosmological "optical" metrics have been proposed, in particular Gordon's optical metric, with modified indices of refraction for manifolds containing "fluids, etc.". These earlier works show that an optical metric on a curved spacetime can be generalized to include absorption by allowing the metric to become complex.

In the perspective of [14], the distorted-geometry model is a departure from the classical geometry model where the Einstein Curvature tensor is the stress-energy-tensor describing the "material contents" of the energy distribution. The distorted-geometry model is rather viewed with the energy-content residing in the warping of the manifold and therefore in its geometric-tensors, with the associated energy content resulting from the creation process which produced the distorted feature in the manifold; the energy is fundamentally manifested in the distorted manifold itself and the "curved empty space" [13] referred to above is a "curved space" devoid of an "external or foreign" causative matter-entity, a first principle representation.

2. Radiation Propagation in the Manifold

Relating to the classical astronomical "redshift" frequency form, it was historically assumed that astronomically observed frequency shifts, Δv, originated from a moving source (the Doppler effect), however the latter-day interpretation is one of an expanding transmission medium (the spacetime manifold) where

$$z \stackrel{\text{def}}{=} redshift\,, \qquad \frac{\nu_{observed}}{\nu_{emitted}} \stackrel{\text{def}}{=} \frac{1}{1+z} \qquad and \qquad \frac{1}{1+z} = \sqrt{\frac{1-\frac{vel}{c}}{1+\frac{vel}{c}}}\,. \tag{1}$$

The "Hubble-velocity (*vel*)" factor [21], thus interpreted and presently accepted as a "space-expansion-velocity" factor, has been experimentally measured at

$$H0 \stackrel{\text{def}}{=} 7.1(10)^4 \frac{m}{\text{sec} * megaparsec}\,.$$

See the encyclopedic website at **Hubble's law** for a comprehensive discussion and illustration of the experimental measurements (scatter plot) and their aberrations or peculiarities.

But consideration of the presence of electromagnetic energy sources in the interstellar and intergalactic media (gas in ionic, atomic, and molecular form, as well as charged dust, cosmic rays and plasma-energy sources), that is energy constituents other than conventional gravitational ingredients, as contributors to universe-energy, would lead to potential sources of radiation absorption and inelastic energy loss, however randomly and anisotropically distributed (a reason for the encyclopedic scatter plot just cited ?). Radiation propagation in and through terrestrial plasma environments have shown the very absorption phenomena we are here advancing [1-9] and being scalable [22], the phenomena could be incorporated into calculations at extra-galactic, or cosmological, dimensional magnitudes, at least insofar as they create a localized (?) substantive transmission-medium. In this work we evaluate the physical plausibility of such an "inelastic-energy-loss", or substantive-manifold, model.

In addition, having previously [14] ascribed the attribute of "curvature" (interpreted as a distortional-concept or elastic-characteristic) to the geometric manifold, we will also advance an explosive creation-process for a distortional-universe by incorporating this additional theorized energy-loss manifold feature.

We enumerate some of the known radiation-energy-loss processes originating from a substantive-medium and postulate a possible phenomenological interpretation of inelastic energy-loss processes as causing radiation-frequency-reduction in the propagating astronomical medium; *for example in the manner of the* **Compton effect** *(observed that when X-rays of a known wavelength interact with atoms, the X-rays are scattered through an angle theta and emerge at a different wavelength related to θ. Although classical electromagnetism predicted that the*

wavelength of scattered rays should be equal to the initial wavelength, multiple experiments had found that the wavelength of the scattered rays was longer (corresponding to lower energy) than the initial wavelength), or in **Brillouin scattering** *(The result of the interaction between the light-wave and the carrier-deformation wave is that a fraction of the transmitted light-wave changes its momentum (thus its frequency and energy) in preferential directions)*,or in **Raman scattering** *(the inelastic scattering of a photon by molecules which are excited to higher vibrational or rotational energy levels), or in the energy-absorbing optoimpulsive- and* **optopiezic-effect** *phenomena*.

Subsequently we construct a phenomenological mathematical representation of the astronomical photon-inelastic-energy-loss-process as a non-linear variation of the established linear energy-loss characterization-functions for particle interactions in nuclear reactions, or in an absorbing medium, as is expressed by the **Bethe formula** for example. A further phenomenological justification or analytical support for the mathematical structure of (1a) is given by Herzfeld [29]. In his studies of absorption of ultrasonic waves in gases and liquids, he asserts "When a plane simple harmonic sound wave is propagated through a medium with relaxation, it is necessary to introduce *absorption*."

He further relates on page 57 [29]; "This process of slow energy exchange between different degrees of freedom is the relaxation phenomenon responsible for excess *absorption* of ultrasonic waves in gases .....and in many liquids.

Call E' the momentary value of the internal energy and $E'(T_{tr})$ the value it would have in equilibrium with external degrees of freedom which are at (temperature) T_{tr}. One then assumes the *relaxation equation* [30]
$-dE'/dt = [\, E' - E'(T_{tr}) \,] * 1/\tau$ which contains as individual constant only the relaxation time τ."

The present function (1a) is analogously stated through a single simple inelastic-energy-loss attenuation-coefficient, $\mu(d) = \mu$, and over a path distance d; $E(d) = h\, \nu(d)$ is defined as the energy-magnitude of the "radiation-energy-component-ν" at path-distance d and $E(0) = h\, \nu(0) \equiv h\, \nu_0$ is defined as the energy-magnitude of the "radiation-energy-component-ν" at path-distance $d = 0$. For this non-linear exponential energy-loss mechanism we therefore write

$$E(d) \stackrel{\text{def}}{=} E(0)\, \exp(-\mu\, d), \tag{1a}$$

or, explicitly for electromagnetic radiation and for astronomical frequency-spectroscopy, with transmission velocity c,

$$h\, \nu(d) = h\, \nu_0 \exp(-\mu\, d)\,; \quad d = c\, t\,. \tag{1b}$$

This formulation is therefore an operational characterization of the radiation (optical) energy exchange process via a mathematical representation other than a modified index of refraction (complex dielectric constant). Such a representation leads to an inelastic/absorption based frequency shift;

$$\frac{\nu(d)}{\nu_0} = \exp(-\mu\, d) = \exp(-\mu s\, c\, t). \tag{2}$$

The individual photon is experiencing inelastic-energy-loss as it propagates through the transmitting medium, a non-**linear energy transfer** process; $dE/dx = -\mu\, E0\, \exp(-\mu\, x) = -\mu\, E$. That is, as the photon loses energy it is less able to transmit further energy to the manifold.

Given this possibility that the universe is populated with electromagnetic energy sources or that the manifold itself is substantive (absorptive), the cosmological energy- or frequency-shifts can be understood as energy-losses to an absorptive medium or to a non-expanding absorptive manifold. Such an absorption/attenuation coefficient allows calculation of the astronomical velocity-factor, although not a velocity in this model. The Hubble-form, $H0$, for the frequency variation as a function of source-to-observer distance and velocity, has been expressed relativistically for a flat-space manifold in equations (3) and (4) where d is defined as the "source to observer distance";

$$\exp(-\mu s\, d) = \frac{1}{1+z}\,, \tag{3}$$

and

$$H0\ d = velocity \quad where \quad \frac{velocity}{c} = \frac{1-\left(\frac{1}{1+z}\right)^2}{1+\left(\frac{1}{1+z}\right)^2} = \frac{\exp(\mu s\ d)-\exp(-\mu s\ d)}{\exp(\mu s\ d)+\exp(-\mu s\ d)} = tanh(\mu s\ d). \tag{4}$$

For the simplest of present modeling, absorptive energy-density sources are assumed uniformly distributed throughout the medium.

We use the Hubble relationship to quantify the absorption coefficient as

$$\mu s \overset{def}{\equiv} \mu C = \frac{1}{d}\ ln[1+z\ ] = 5.36\ (10)^{-26}\ m^{-1}\ ,$$

normalized at

$d = c\ Age \overset{def}{\equiv} d_{\mu C(z)}$, where $z \sim 1089$ (defined from the cosmic microwave background shift).

The "absorption" distance-redshift (z) functions and the "Hubble" distance-redshift functions are displayed in Figure.1 where the distance-z functions are expressed in (4) for the "Hubble" distance and (3) for the "absorption" distances, with

$\mu s \overset{def}{\equiv} \mu c = 0.770\ (10)^{-26}\ m^{-1}\ ,$ normalized at $z = 0.1\ \left(d \overset{def}{\equiv} d_{\mu c(z)}\right)$

and $\mu s \overset{def}{\equiv} \mu s = 2.33\ (10)^{-26}\ m^{-1}\ ,$ normalized at $z = 19.5\ (d \overset{def}{\equiv} d_\mu s(z)\ ).$ (5)

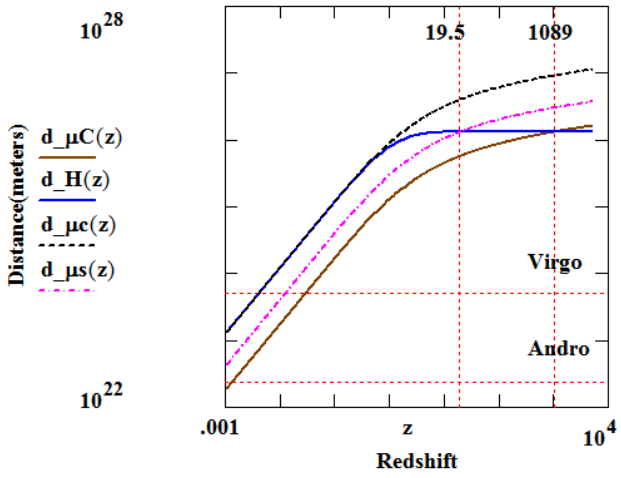

Figure 1. Distance (source to observer)/frequency-change profiles. Absorption distance *d_μC(z)*-vs-*z* (bold-brown), Hubble distance *d_H(z)*-vs-*z* (bold-blue), Absorption distance *d_μc(z)*-vs-*z* (dash-black) and Absorption distance *d_μs(z)*-vs-*z* (dadot-magenta). Virgo is the defined galaxy-cluster distance at 16.5 megaparsecs and Andro is the defined Andromeda galaxy-distance at 0.78 megaparsecs. The redshift-z at 1089 is the CMB (cosmic microwave background) redshift.

A distance (universe radius) prediction for the *d_μc(z)* profile is approximately 7 times the prediction for the Hubble function value *d_H(1089)*.

A "physical universe under expansion" interpretation of increasing z-data is here fundamentally associated with larger frequency (z) shifts arising from longer radiation-absorption paths, and calculable with (6);

$$Source\ observation\ radius = c\,t = d = -\frac{1}{\mu s}\ln\left(\frac{1}{1+z}\right). \tag{6}$$

Besides fundamental differences with distance and time interpretations, we suggest here that experimental astronomical data at the extremes can be understood within, or as part of, the presently-constructed absorptive (electromagnetic-component)-universe, or an absorptive spacetime-manifold-model, and therefore the need for incorporation of an hypothesized additional dark-energy component to describe a "universe under expansion" behavior would be unwarranted (see (2) through (6)).

If a second absorptive species is present in the medium, resulting in a departure from the simpler uniformly-distributed energy-density characterization, then mathematical fitting of the z-behavior at both distance extremes is possible. We have incorporated such energy-density representations according to the absorption-coefficient *μ(d)* constructions in (7)-(9):

$$\mu s \overset{\text{def}}{\equiv} \mu d2 = d20\left(1 + d21\left(\frac{d}{d0}\right)^2\right),\quad d20 = 0.73\,(10)^{-26}\,m^{-1},\quad d21 = 6.4\quad and\ \ d0 = \frac{c}{H0}. \tag{7}$$

$$\mu s \overset{\text{def}}{\equiv} \mu d6 = d60\left(1 + d61\left(\frac{d}{do}\right)^6\right),\quad d60 = 0.77\,(10)^{-26}\,m^{-1}\quad and\quad d61 = 7.0\ . \tag{8}$$

$$\mu s \overset{\text{def}}{\equiv} \mu e = E0\left(1 + e^{d(z)E1}\right),\qquad E0 = 0.34\,(10)^{-26}\,m^{-1}\text{and}\quad E1 = 2.1(10)^{-26}\,m^{-1}. \tag{9}$$

These "absorption" distance-redshift (*z)* functions, the "Hubble" distance-redshift function and the absorptive energy-density functions are displayed in Figures 2 and 3.

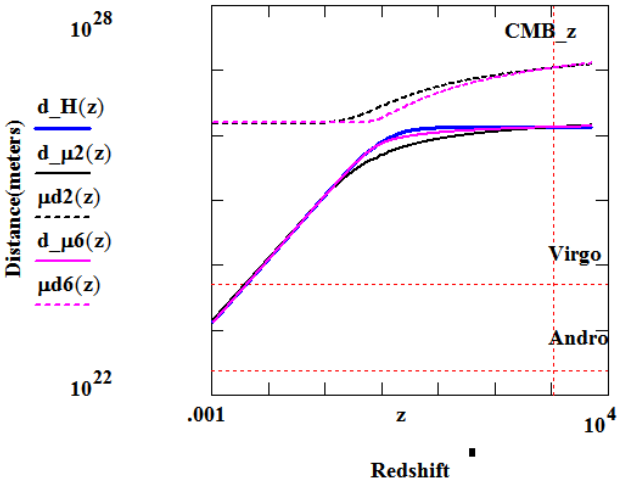

Figure 2. Distance (source to observer)/frequency-change profiles. Absorption distance *d_μ2(z)*-vs-*z* (bold-black), Hubble distance *d_μH(z)*-vs-*z* (bold-blue) and Absorption distance *d_μ6(z)*-vs-*z* (bold-magenta) are illustrated. The Absorption coefficient *μd2(z)*-vs-*z* (dash-black) and Absorption coefficient *μd6(z)*-vs-*z* (dash-magenta) are displayed in units of m^{-1} and multiplied by a factor of 10^{52} for display purposes. Virgo, Andro and CMB_z are defined in Figure caption 1.

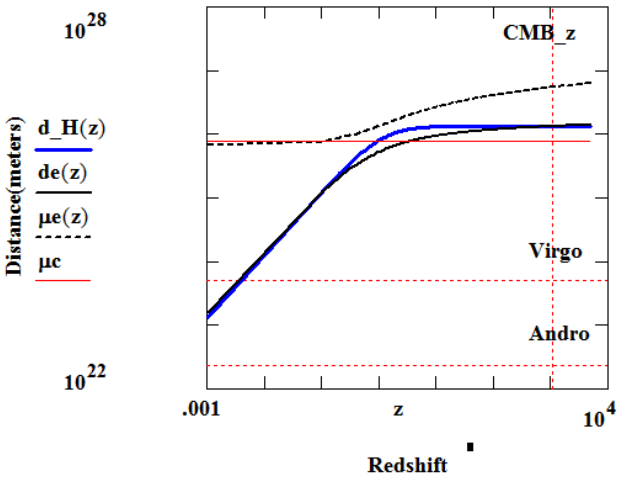

Figure 3. Distance (source to observer)/frequency-change profiles. Absorption distance *de(z)*-vs-*z* (bold-black) and Hubble distance *d_μH(z)*-vs-*z* (bold-blue) are displayed. The Absorption coefficient *μe(z)*-vs-*z* (dash-black) and the constant-density coefficient *μc* (red) are displayed in units of m^{-1} and multiplied by a factor of 10^{52} for display purposes. Virgo, Andro and CMB_z are defined in Figure caption 1.

We display, on logarithmic scales in Figure 4, these second order absorption coefficients as a function of distance; this illustration supports the hypothesized condition of an earlier denser universe, that is, radiation propagation through a denser medium (from an earlier time and a longer path) produces a greater frequency-shift (energy-loss). All (a non-exhaustive set) of the functional constructs (*μe(z), μd2(z)* and *μd6(z)*), presently utilized to produce numerical Hubble-distance agreement at the larger-distance z-value (z = 1089), exhibit an early-time larger absorption coefficient.

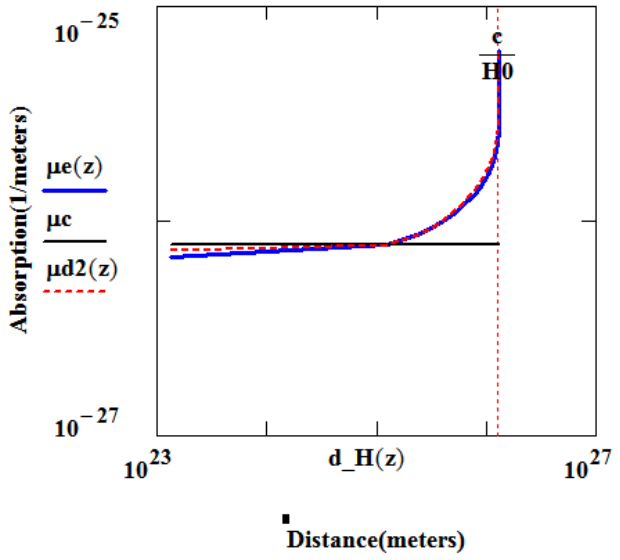

Figure 4. Absorption-coefficient/Distance profiles. Absorption coefficient *μe(z)*-vs-distance (bold-blue), Absorption coefficient *μd2(z)*-vs-distance (dash-red) and Absorption coefficient *μc(z)*-vs-distance (bold-black) are displayed.

In the absence however of an independent distance- or absorption-coefficient- "known state-variable", the radiation-absorption universe model only produces the product-variable "$\mu\, d$". Therefore either the distance-result quoted from (5) with $\mu s = \mu c = (c\ Age)^{-1}$, and assuming $d_H(z = 0.1)$ is physically acceptable, or the absorption-coefficient result quoted from (7-9), would be allowable.

Although many experiments [23-26] have been performed in an attempt to detect the relative motion of radiative-energy through a stationary "luminiferous aether (aether wind)" and to test the tenets of special relativity, the experiments have shown uncertainties (best @ $\leq 10^{-8}$) [26] many orders of magnitude greater than that needed to relate to the magnitude of the attenuation coefficient μs. The small magnitude of the astronomical light-source frequency-change effect (now depicted as due to spatial expansion but here modeled as an inelastic electromagnetic-radiation energy-loss) is illustrated by the following ; at earth to moon distances ($4*10^8$ m) the absorptive loss ($1 - exp(-\mu s\ d)$) would be ~ $(10)^{-17}$ and difficult to detect experimentally, however this experimental-measurement challenge exists for all cosmological data acquisition including the spatial-expansion frequency-change model, where the Hubble shift is $\Delta v/v = 3(10)^{-18}$ at earth to moon distances (actually the "spatial-expansion Hubble-shift" model (phenomenon) is considered not applicable at "local" distances). We have of course intentionally mimicked or modeled the same astronomical data as for the spatial expansion model.

If the intergalactic (as well as intragalactic) medium and associated inelastic-energy loss processes could be simulated in the laboratory then radiation-absorption characteristics could perhaps be determined and scaled to cosmological distances and densities. Other potentially meaningful experimental undertakings are not known at this time. Historically and alternatively, proponents of plasma-universe models are hopeful [22] of success although these models could also be considered absorption-models.

The vanishingly small character of an absorption coefficient necessary to describe the intergalactic spatial electromagnetic energy sources which will produce the astronomically-measured light-source frequency-shifts would seem however to support the absorption-model concept.

3. Distortional Energy Decay

For a distorted-geometry spherical universe model, the observational isotropic perspective would be represented by an observer at $r = 0$, the original center-location of the immense spatial distortion and the spherical center of the subsequent explosively propagating shock-wave. The observer would actually be looking toward the younger (later) created elements from the wave with radiation from said emitting elements having propagated through the longer absorbing path of the manifold; the observer would be sitting at the oldest part of the shock-wave created universe. Whether the energy-seeded and therefore transmission-modified local manifold's absorption properties would further impact the manifold attenuation-coefficient is not addressed at this point although matter-energy absorption in the manifold is treated with a separate and different attenuation-coefficient from radiation-energy absorption.

With this perspective of the absorption-induced energy-density components of the manifold, we display in Figure 5 the results of such calculations wherein matter-energy sources are assumed detectable via radiation emission for the observer at time t; $t = Age$ would apply for a present-day observer. The energy-density equations are taken from the development in the section, (18a) for ρU_M.

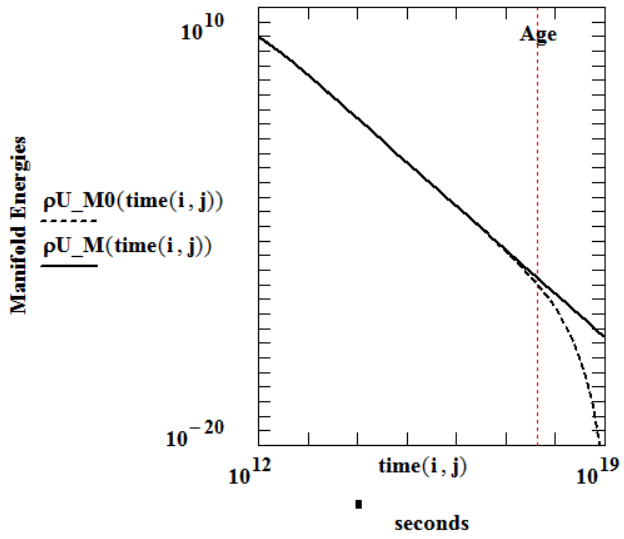

Figure 5. Ordinary-matter ("as-deposited/absorbed" and "as-observed/altered") energy-density profiles (in *Joules/m*^{3}). *ρU_M* designates the ordinary matter "as-deposited" profile (Eq.15a) while *ρU_M0* designates the path-altered or "as-observed" profile (Eq.15a) $\star$ *exp(-μs c t).*

The deposited energy-density functions inherently contain an equilibrating element through incorporation of the spherical volume-expansion representation in (18a).

In Figure 6 we show the calculational results responsible for the deposited-energy temperature functions of (21); the post-Age time evolution of the radiation component is also shown.

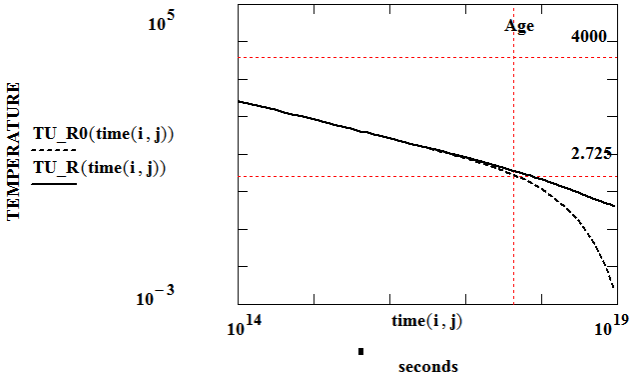

Figure 6. Radiation-observed temperature-profiles (*TU_R0* for path-altered and *TU_R* non-path-altered) of the wave-deposited radiation component; note the post-age development.

We depart from the current Big Bang/singularity model and utilize the classical Stefan-Boltzmann equations to describe the time-evolution of a presently engendered massive, unstable (radiating as a blackbody) geometric-distortion; we thereby create an energy-time development profile (an explosive event) for the unstable structure. The mass-energy decay time profile (Stefan-Boltzmann) is,

$$P = \frac{dU}{dt} = -(\sigma T^4)\, A(r) \quad \text{and} \quad A(r) = 4\pi\, r^2\,, \tag{10}$$

where the total radiating energy is represented in *U*, or

$$\frac{dU}{dt} = -c(\pi\rho)^{\frac{1}{3}}\left(\frac{3U}{4}\right)^{\frac{2}{3}} \tag{11}$$

with

$$U = the\ distortional\ energy\ @\ constant\ density, \text{ leading to } \quad U(t) = -3\,\frac{\pi\rho}{16}(c\,t)^3 + U0\,. \tag{12}$$

For a geometric (gravitationally-formulated) maximum ρ, that is, using the Schwarzschild gravitational radius ≡ r_G as a measure of the geometric-curvature ($1/\ r_G$) and equating it to the "maximum-curvature" [14], which is a Fermi-constant derived curvature for geometrically-distorted structures, a maximum mass-energy-density is calculated;

$$r_G = 2\,\kappa_G M_G = \frac{G}{c^4}\,M_G$$

and

$$\rho = M_G\left[\frac{4\pi}{3}\left(\frac{G}{c^4}\,M_G\right)^3\right]^{-1} = \left[\frac{4\pi}{3}\frac{G}{c^4}\right]^{-1}\frac{1}{(r_G)^2} = \left[\frac{4\pi}{3}\frac{G}{c^4}\right]^{-1}\frac{1}{r_min^2} = 4.1678(10)^{80}\,\frac{J}{m^3},$$

associated with a gravitational coupling constant and where

$$\frac{1}{r_min^2} = (u0B\,\pi)^2\left(\frac{3\,GF}{MW}\right)^{-2/3}. \tag{12a}$$

For comparison, as calculated from the geometric (EM (electromagnetic)-formulated) maximum ρ for the W^- boson [14],

$$\rho_{geo_{boson}} \stackrel{\text{def}}{=} \rho GF = \frac{u0B^3}{GF}\left(MW\,\frac{\pi}{2}\right)^2 = 1.687(10)^{47}\,\frac{J}{m^3},$$

associated with an electromagnetic coupling constant and

$$Temp_{geo_{boson}} = \left(\frac{\rho GF}{4}\,\frac{c}{\sigma}\right)^{\frac{1}{4}} = 3.86\,(10)^{15}\,K\,. \tag{12b}$$

We have posited for this radiating geometrically-distorted structure, the maximum geometric distortional density $\underline{\rho}$ expressed in (12a), where *GF* is the Fermi constant, *MW* is the W^- boson mass-energy and *u0B* = 1.807 [14].

A final extinction time, wherein all of the structural energy has been depleted and converted to wave-energy, is reached at

$$tf = \frac{1}{c}\left(\frac{16\,U0}{3\,\rho\,\pi}\right)^{1/3}, \tag{13}$$

thereby producing a propagating spherical shock-wave with a time-width of *tf* and inherited blackbody features; we assume a shock-wave velocity = *c* and apply such a descriptive-development to characterize the exploding distortion with a mass-energy-magnitude equal to the total-universe-energy *U0*. Construction of the "*total-universe-energy"* is accomplished by ascribing to the blackbody sphere the energy content presently and experimentally observed as "*ordinary + dark*" matter-energy; that is, we use a *radius = c*Age* and an energy-density equal to the *"observational(ord) + dark" matter-energy-density = 5.78 (10)$^{-9}$ J/m^3* to define the "*total-universe-energy"*; *"ord"* = 4.9 % and *"dark"* = 26.8 %. In that case with *U_univ ≡ U0 = 5.38(10)^{70} Joules, tf = 4.18(10)$^{-12}$ seconds.* If *U_univ = 2.75(10)^{71} Joules, tf = 2.14(10)$^{-11}$ seconds.*

Displayed in Figure 7 is the time profile of the emerging shock-wave the instant after extinction of the originating spacetime-distortional. The profile is constructed to illustrate the immediate effects of the expanding geometry on the energy profile.

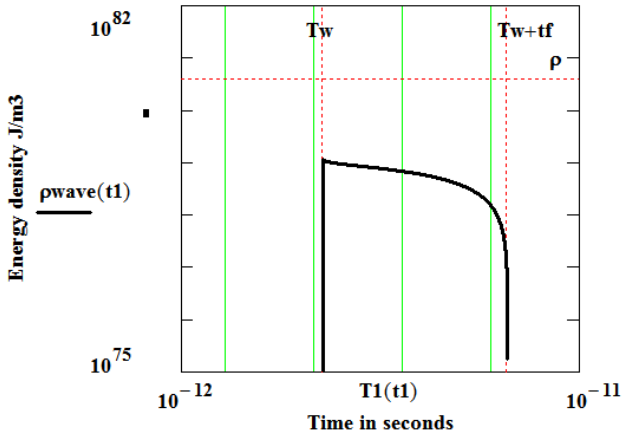

Figure 7. Shock-Wave energy-density function (*J/m*^{3} with geometrical reduction = *1/(4π r*^{2}) versus time on the abscissa. Time *Tw* is equal to time *tf*, the extinction time, in this graph and therefore the profile is one of the newly emerging wave.

The emergent spherical shock-wave expands radially through the spacetime manifold at velocity *c*, seeding the manifold and culminating (an exponentially decreasing culmination) at the ultimate physical boundary characterized by the attenuation coefficient. Such a universe, a propagating energy-shell creating an energy-seeded internal sphere, complicates geometric characterization but the spherical matter-energy-density, radially defined by the shell boundary, would represent a "time-changing geometric descriptor" from *closed (contracting)* ($\Omega = \rho_U_{matter}/\rho_{critical}$ = *4.21(10)*^{59} *@ tf*) to *open (expanding)* (Ω = *1 @ 1.0064 Age*); $\rho_{critical}$ =*3H0*^{2}*/8πG* . The "geometric characterization" of the manifold is therefore not explicitly represented.

The radius of this radiating blackbody and its associated temperature are

$$Radius = \left(\frac{3}{4\pi}\frac{U0}{\rho}\right)^{\frac{1}{3}} = 3.14(10)^{-4}\ meters\ \ and\ \ \ Temp = \left(\frac{c}{4\sigma}\rho\right)^{1/4} = 8.62(10)^{23}\ K\ , \tag{14}$$

where σ is the Stefan-Boltzmann constant and ρ is the geometric-maximum-density specified in (12a).

Because the radiation component associated with the wave is small *(~10*$^{-6}$) compared to the matter component, it has been omitted from the *U0* calculation. Experimental values [27-28] for these energy-density components are incorporated as ρU_{matter} = *5.79(10)*$^{-9}$ *J/m*^{3} (reported at Age) representing "ordinary (baryonic) + dark" matter and

$$\rho U_{radiation} = (2.725)^4\ \frac{4\sigma}{c} = 4.1934(10)^{-14}\ \frac{J}{m^3}\ \ (reported\ @\ Age). \tag{15}$$

We now advance and investigate the effects of the additional manifold feature developed in the previous section, an energy-absorbent or attenuating characteristic. Energy production in the manifold comprises both the wave's characteristic as energy source and the absorbent medium's characteristic ability to receive (absorb) the energy. Energy and energy-density equations for the resultant wave are expressed as,

$$\rho Wave_{ord-matter}(t) = U0\ f_{ord}\ (vol_wave(t))^{-1} \exp(-\mu a\ c\ t)\ ,$$

$$\rho Wave_{dark-matter}(t) = U0\ f_{dark}\ (vol_wave(t))^{-1}\ \exp(-\mu a\ c\ t)$$

and

$$\rho Wave_{radiation}(t) = U0\ f_{radiation}\ (vol_wave(t))^{-1} \exp(-\mu s\ c\ t)$$

where

$$vol_wave(t) = \frac{4\pi}{3} c^3\ (3\ tf\ t^2 + 3\ tf^2 t + tf^3). \tag{16}$$

After integrating over the volume extent of the wave-shell,

$$wave\ shell\ volume = \left[\frac{1}{tf^3} \int_t^{t+tf} \frac{1}{\frac{1}{3} + \frac{\tau}{tf} + \left(\frac{\tau}{tf}\right)^2} \tau^2\ d\tau \right]$$

and

$$U0\ f_{matter}\ [wave\ shell\ volume]^{-1} \exp(-\mu a\ c\ t) = UWave_{matter}(t) \tag{17}$$

The matter and radiation energy components become

$$UWave_{ord_matter}(t) = U0\ f_{ord}\ \exp\big(-\mu a\ c\ (t)\big),$$
$$UWave_{dark_matter}(t) = U0\ f_{dark}\ \exp\big(-\mu a\ c\ (t)\big)$$

and

$$UWave_{radiation}(t) = U0\ f_{radiation}\ \exp\big(-\mu s\ c\ (t)\big). \tag{17a}$$

With respect to the radiation component of the wave and its deposited/absorbed energy in the manifold, or left in the wake of the propagating wave (specified experimentally through discovery of the cosmic-wave-background-radiation), $f_{radiation} = 7.28(10)^{-6}$. The deposited manifold energy densities are then

$$\rho U_{ord-matter}(t) = U0\ f_{ord} \left(\frac{4\pi}{3}(c\ t)^3\right)^{-1} (1 - \exp(-\mu a\ c\ t)\ )$$
$$\rho U_{dark-matter}(t) = U0\ f_{dark} \left(\frac{4\pi}{3}(c\ t)^3\right)^{-1} (1 - \exp(-\mu a\ c\ t)\ )$$

and

$$\rho U_{radiation}(t) = U0\ f_{radiation} \left(\frac{4\pi}{3}(c\ t)^3\right)^{-1} (1 - \exp(-\mu s\ c\ t)\ ). \tag{18}$$

Deposited-energy-equations are, similarly,

$$U_{ord_matter}(t) = U0\ f_{ord}\ (1 - \exp(-\mu a\ c\ t)),$$
$$U_{dark_matter}(t) = U0\ f_{dark}\ (1 - \exp(-\mu a\ c\ t))$$

and

$$U_{radiation}(t) = U0\ f_{radiation}\ (1 - \exp(-\mu s\ c\ t)). \tag{18a}$$

In the distorted-space narrative [14], the matter-like distortions include both electromagnetic and gravitational structures, via a composite coupling constant, which we have detailed as "*observational* or *ordinary*" plus "*dark*" matter. Radiation attenuation has been treated with the absorption coefficient μs, however, matter, or mass-energy, is here treated with an independent attenuation factor μa. This factor is constrained or determined from the time "*tel"*

that the wave energy-density reaches the extreme energy-density expressed as the minimum energy-density for distortional-electron formation [14];

$$\rho U_{electron} = U0 * vol_wave(tel)^{-1} \exp(-\mu a\ c\ tel) \quad \text{or} \quad \mu a = -\frac{1}{c\ tel} ln\left(\frac{\rho U_{electron}\ vol_{wave(tel)}}{U0}\right)$$

where

$$\rho U_{electron}\left(\frac{J}{m^3}\right) = (me\ c^2)^4 \frac{3}{\pi\ \alpha fs}\left(\frac{UM0}{\hbar\ c}\right)^3 = 5.09(10)^{26}\ \frac{J}{m^3}\ , \quad UM0 = 1.40$$

and

$$\alpha fs = fine\ structure\ constant\ . \tag{19}$$

The propagating wave's matter-temperature at this electron mass energy density is

$$Wave_Temp_{electron} = \left(\rho U_{electron}\frac{c}{4\sigma}\right)^{1/4} == 2.86\ (10)^{10}\ K.$$

We set the time *"tel" ="recombination time"= 1.19(10)[13] s* (from the prevailing cosmological model, the Big Bang theory) as an approximation to the "electron-distortional-structure formation-end-time", which leads to μa = *1.69(10)[-21] m[-1]* and a radiation-sphere temperature

$$Sphere_{Temp_{radiation}}(tel) = \left(\rho U_{radiation}(tel)\frac{c}{4\sigma}\right)^{\frac{1}{4}} = 3962\ K.$$

The radial radiation-expansion volume-factor (18) is f_{volume} = *0.067*. Using the mixing function value (radial radiation-expansion volume-factor) ascribed to the radiation temperature at *time=Age*, the calculated Sphere_*Temp* is *750 K*.

The fixing of μa allows determination of the starting time for distortional-matter production, that is for production of a structural-energy-density to mimic the W^- boson [14], which represents the maximum distortional-curvature for distortional-matter production in the wave;

$$\rho U_{Wboson} = \rho GF = U0 * vol(tWB)^{-1} \exp(-\mu a\ c\ tWB). \tag{20}$$

This calculation leads to *tWB = 1.34(10)[4] s*, although the exponential factor contributes insignificantly; the wave has propagated radially to *r = 4.02(10)[9] km*.

Radiation deposition, or absorption, is assumed to initiate immediately at *t = tf* during the creation process, accompanied by, a "radiation-expansion" from the wave (a shell at radial thickness = c_*tf) into the spherical spatial manifold; this "equilibration-expansion" is expressed as the "*volume-change ratio* = $\left[{}^{4\pi}/_{3}\,(c\ t)^3\right]/vol_wave(t)$" with an accompanying "mixing process function" expressed as a "pseudo volume-radius reduction". The temperature function, $TU_{radiation}$, (18), evaluated at *t = Age*, with the observational-absorption function *exp(-μs c t)*, expresses this result;

$$TU_{radiation}(Age) = \left[\frac{c}{4\sigma}\ \rho U_{radiation}(Age)\right]^{0.25} = 2.725\ K,$$

$$\rho U_{radiation}(Age) = \begin{bmatrix} U0\ f_{radiation}\left(\frac{4\pi}{3}\left(c\ Age\ f_{volume}\right)^3\right)^{-1} \times \\ \times\ (1 - \exp(-\mu s\ c\ Age)\ )\exp(-\mu s\ c\ Age) \end{bmatrix}^{0.25}, \quad \text{and} \quad f_{volume} = 0.616\ . \tag{21}$$

The radial radiation-expansion volume-factor (*radius = c t*) is apparently overstated and a correction factor f_{volume} has been added (a radial-reduction to 0.616 *c t*) to produce temperature agreement.

In summation, creation of matter is understood to take place after the wave has diluted to the "maximum for particle formation" at *ρWB*, the energy-density associated with the maximum distortional-geometric-curvature and at a time $tWB = 1.34(10)^{4}$ *s*. Particle creation continues to a wave energy-density limit for electron formation, $tel = 1.19(10)^{13}$ *s*. Radiation creation is considered possible at all energy-density levels. Attributes of the decaying wave-energy-densities are shown in Figure 8 and Figure 9.

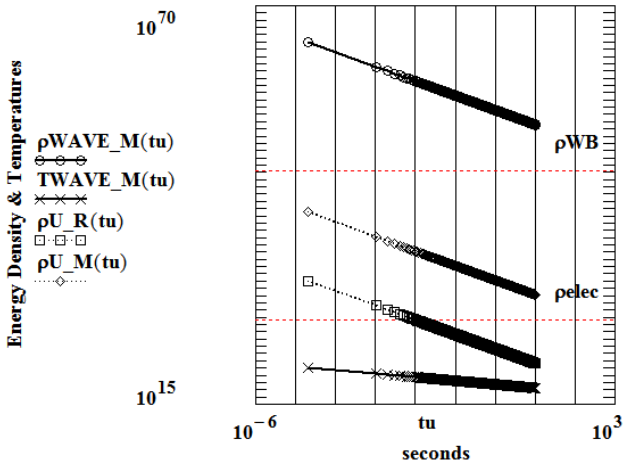

Figure 8. Matter shock-Wave (⊙) energy-density (J/m^3) and temperature functions (*K*) (⊠; wave) versus time on the abscissa. Deposited energy-densities (J/m^3) functions (⊡, radiation and ⧄, matter) versus time on the abscissa. The critical energy-densities, *ρWB* (W-boson) and *ρelec* (electron), already established and cited, are noted.

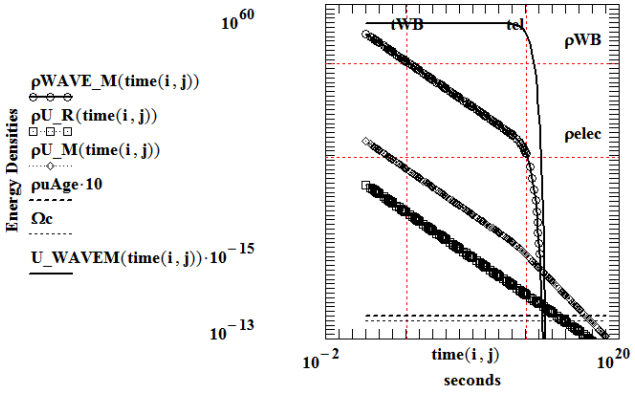

Figure 9. Matter shock-wave energy-density (J/m^3) functions (⊙; *ρWAVE_matter*) versus time on the abscissa. Deposited energy-density (J/m^3) functions (⧄ for matter and ⊡ for radiation) versus time on the abscissa. The critical boson energy-density *ρWB* and the critical electron energy-density *ρelec* in the wave are shown. The equilibrated radiation-energy-density function *ρU_rad* is depicted as (---) and the critical energy-density as (……). Also shown is the total mass-energy in the wave *U_WAVEM* (——).

It is apparent from the initial spatial deposition and distribution of the wave-energy that energy equilibration/mixing processes (via volume-expansion already discussed in the section "Radiation Propagation in the Manifold") ensue to achieve a final spatially-independent energy distribution in such a universe.

Decaying wave energies are illustrated in Figure 10. Accumulating manifold energies are shown in Figure 11 and

Figure 12. The matter-energy and radiation-energy depositions displayed in Figures 11 and 12 have reached saturation at times ~ 10^{18} seconds.

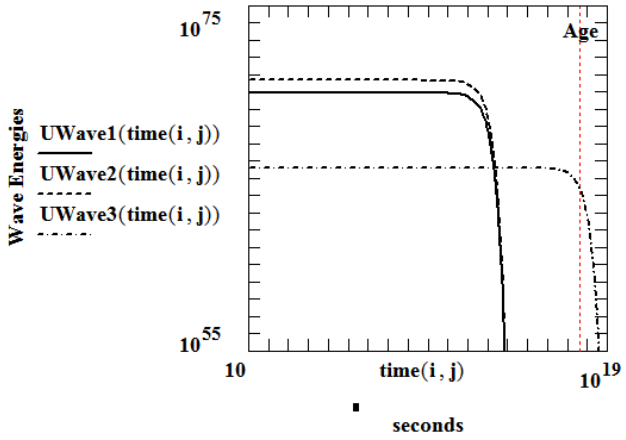

Figure 10. The depleting matter-wave-energies (*UWave* (Eq.12a) in *Joules*) (solid = 1 = *ord_matter*, dash = 2 = *dark_matter*) and the radiation-wave-energies (dadot = 3 = *rad*) vs later times in the wave's life.

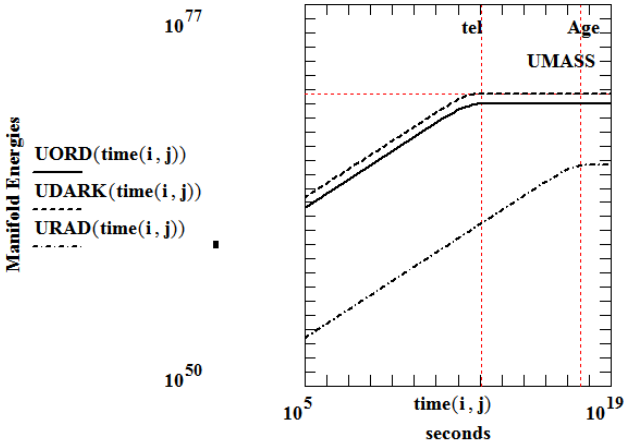

Figure 11. The accumulating manifold energies (*Joules*) (solid = *ord_matter*, dash = *dark_matter*, dadot = *radiation*) vs time in the wave's life. *time (i,j) = j(10)^{i} . UMASS = U0*.

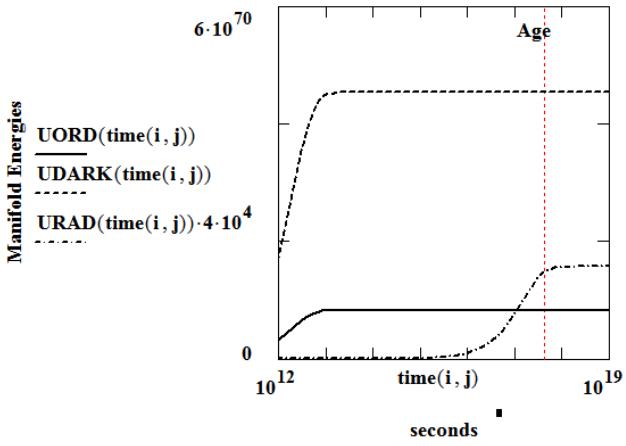

Figure 12. The accumulating manifold matter energies (*Joules*) (solid = *ord-matter*, dash = *dark-matter*) and the accumulating manifold radiation energy (*Joules*) (dadot) vs time in the wave's life.

4. Conclusions

It has been posited in the present work that the classical astronomically observed electromagnetic frequency shifts can be interpreted as produced by absorption and inelastic energy-loss in a substantive spacetime manifold or as produced by inelastic energy-loss absorption from universe-sited electromagnetic energy sources. The presence of a gravitational dark-energy component throughout the universe may be illusory if extreme radiation-shifted astronomical phenomena are interpreted as originating from such absorptive energy sources or an absorptive geometric manifold. Finally, we have incorporated such absorption concepts to describe an explosively-driven energy-production-model of a distortional-universe to characterize the time-development, distances, energy-densities and matter and radiation production within the manifold.

Acknowledgments

Since this work is a continuation of the fundamental endeavor expressed in [14], we again acknowledge the creative critique offered by, Dr. J T Grissom for his valuable suggestions for technical clarification and material emphasis and, the helpful corrective conceptual commentary of Dr. J D Weiss, relative to that work.

References

[1] Alfvén, H., "Cosmology—Myth or Science?" J. Astrophys. Astr., vol. 5, pp. 79-98, 1984.
[2] LiXin Guo and JiangTing Li, Physics of Plasmas, vol. 24, 022108, 2017.
[3] Laroussi, M., "Interaction of microwave with atmospheric pressure plasmas," Int. J. Infrared Millimeter Waves, vol. 16, pp. 2069–2083, 1995.
[4] Bliokh, Y.P, Felsteiner, J. and Y. Z. Slutsker, Y.Z., "Total absorption of an electromagnetic wave by an overdense plasma," Phys. Rev. Lett., vol. 95, 165003, 2005.
[5] Laroussi, M. and Roth, J.R., "Numerical calculation of the reflection, absorption, and transmission of microwaves by a nonuniform plasma slab," IEEE Trans. Plasma Sci., vol. 21(4), pp. 366–372, 1993.
[6] Petrin, A.B., "Transmission of microwaves through magnetoactive plasma," IEEE Trans. Plasma Sci., vol. 29(3), pp. 471–478, 2001.
[7] Xi, Y.B. and Liu, Y., "Effect of electron density profile on power absorption of high frequency electromagnetic waves in plasma," Phys. Plasmas, vol. 19, 073301, 2012.

[8] Cerri, G., Moglie, F., Montesi, R., Russo, P., and Vecchioni, E., "FDTD solution of the Maxwell–Boltzmann system for electromagnetic wave propagation in a plasma," IEEE Trans. Antennas Propag., vol. 56, pp.2584–2588, 2008.
[9] Guo, B. and Wang, X.G., "Power absorption of high-frequency electromagnetic waves in a partially ionized magnetized plasma," Phys. Plasmas, vol. 12, 084506, 2005.
[10] Ciufolini, I. and Wheeler, J. A. , Gravitation and Inertia, USA, Princeton University Press, 1996.
[11] Wheeler, J. A., Phys. Rev., vol. 97, p.511, 1955.
[12] Wheeler, J. A., "Logic, Methodology, and Philosophy of Science", Proc. 1960 International Congress, USA, Stanford University Press, p.361, 1962.
[13] Clifford, W. K., Proc. Cambridge philosophical society vol.2, p.157, 1876.
[14] Koehler, D. R., Indian Journal of Physics, vol. 87, p.1029, 2013.
[15] Koehler, D. R., The Distorted Universe: From Neutrinos to the Cosmos, The Theory of Nothingness, Kindle: ASIN B00TG26Q7Y, 2015.
[16] Gordon, W., Annals of Physics, vol. 22, p. 421, 1923.
[17] Chen, B. and Kantowski, R., Phys. Rev.; vol. D 78: 044040, 2008.
[18] Chen, B. and Kantowski, R., Phys. Rev., vol. D 79: 104007, 2009.
[19] Chen, B. and Kantowski, R., Phys. Rev., vol. D 80: 044019, 2009.
[20] Lima, J. A. S., Cunha, J. V. and Zanchin, V. T., Astrophysical Journal Letter, vol. 742 : 26, 2012.
[21] Lemaître, G., Annals of the Scientific Society of Brussels, vol. 47A: 41, 1927.
[22] Alfvén, Hannes, "On hierarchical cosmology", Astrophysics and Space Science, vol. 89 (2), pp.313–324, 1983.
[23] Braxmaier, C., Müller, H., Pradl, O., Mlynek, J., Peters, J. A. and Schiller, S., Phys. Rev. Lett., vol. 88: 010401, 2002.
[24] Mansouri, R. and Sexl, R.U., Gen. Rel. Gravit., vol. 8, p. 809, 1977.
[25] Müller, J., Nordtvedt, K., Schneider, M. and Vokrouhlicky, D., Proceedings of the 11th International Workshop on Laser Ranging Instrumentation, vol. 10, p. 216, 1999.
[26] Wolf, P., Tobar, M. E., Bize, S., Clairon, A., Luiten, A. N. and Santarelli, G., General Relativity and Gravitation, vol. 36, p. 2351, 2004.
[27] Davies, P., The Goldilocks Enigma, First Mariner Books, vol. 43, 2006.
[28] http://map.gsfc.nasa.gov/universe/uni_matter.html.
[29] Herzfeld, K. F. and Litovitz, T. A., Absorption and Dispersion of Ultrasonic Waves, Academic Press, 2013.
[30] Herzfeld, K. F. and Rice, F. O., Phys. Rev. vol. 81, p.891, 1928.

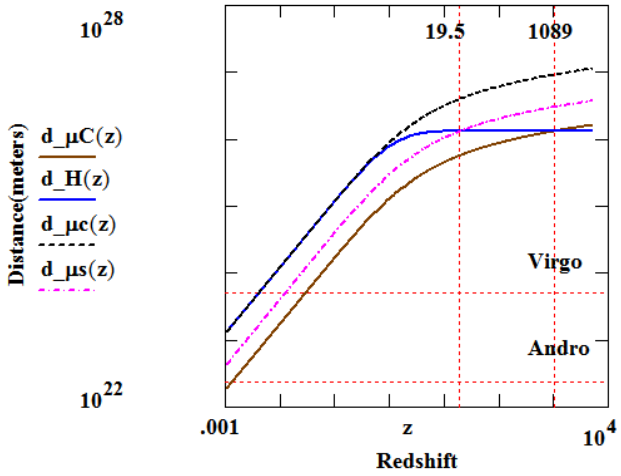

Figure 1. Distance (source to observer)/frequency-change profiles. Absorption distance *d_μC(z)*-vs-*z* (bold-brown), Hubble distance *d_H(z)*-vs-*z* (bold-blue), Absorption distance *d_μc(z)*-vs-*z* (dash-black) and Absorption distance *d_μs(z)*-vs-*z* (dadot-magenta). Virgo is the defined galaxy-cluster distance at 16.5 megaparsecs and Andro is the defined Andromeda galaxy-distance at 0.78 megaparsecs. The redshift-z at 1089 is the CMB (cosmic microwave background) redshift.

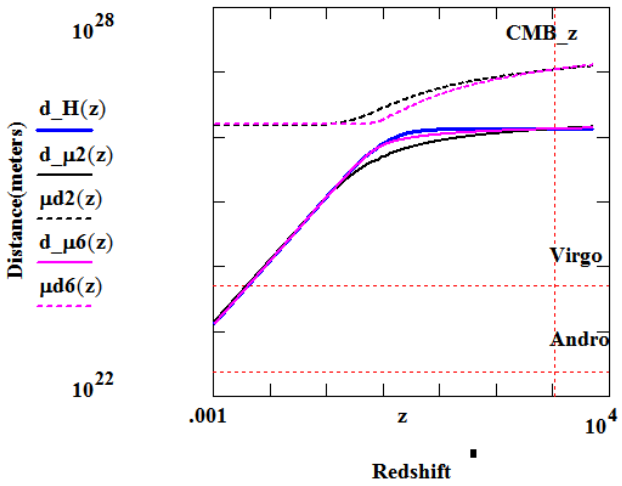

Figure 2. Distance (source to observer)/frequency-change profiles. Absorption distance *d_μ2(z)*-vs-*z* (bold-black), Hubble distance *d_μH(z)*-vs-*z* (bold-blue) and Absorption distance *d_μ6(z)*-vs-*z* (bold-magenta) are illustrated. The Absorption coefficient *μd2(z)*-vs-*z* (dash-black) and Absorption coefficient *μd6(z)*-vs-*z* (dash-magenta) are displayed in units of m^{-1} and multiplied by a factor of 10^{52} for display purposes. Virgo, Andro and CMB_z are defined in Figure caption 1. .

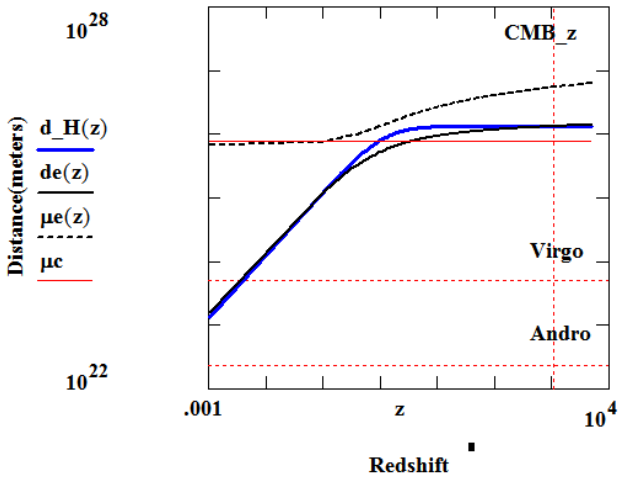

Figure 3. Distance (source to observer)/frequency-change profiles. Absorption distance *de(z)*-vs-*z* (bold-black) and Hubble distance *d_μH(z)*-vs-*z* (bold-blue) are displayed. The Absorption coefficient *μe(z)*-vs-*z* (dash-black) and the constant-density coefficient *μc* (red) are displayed in units of m^{-1} and multiplied by a factor of 10^{52} for display purposes. Virgo, Andro and CMB_z are defined in Figure caption 1.

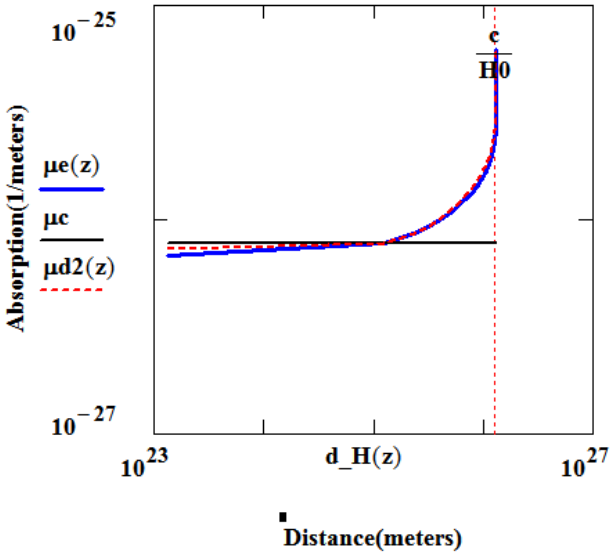

Figure 4. Absorption-coefficient/Distance profiles. Absorption coefficient *μe(z)*-vs-distance (bold-blue), Absorption coefficient *μd2(z)*-vs-distance (dash-red) and Absorption coefficient *μc(z)*-vs-distance (bold-black) are displayed.

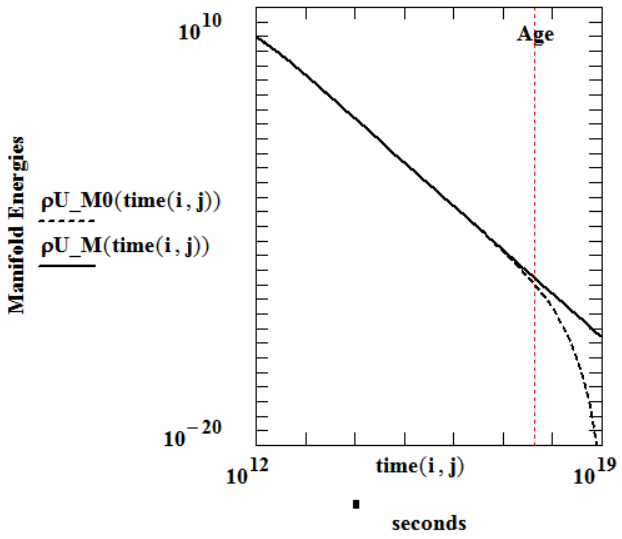

Figure 5. Ordinary-matter ("as-deposited/absorbed" and "as-observed/altered") energy-density profiles (in *Joules/m*^{3}). *ρU_M* designates the ordinary matter "as-deposited" profile (Eq.15a) while *ρU_M0* designates the path-altered or "as-observed" profile (Eq.15a) $*$ *exp(-μs c t).*

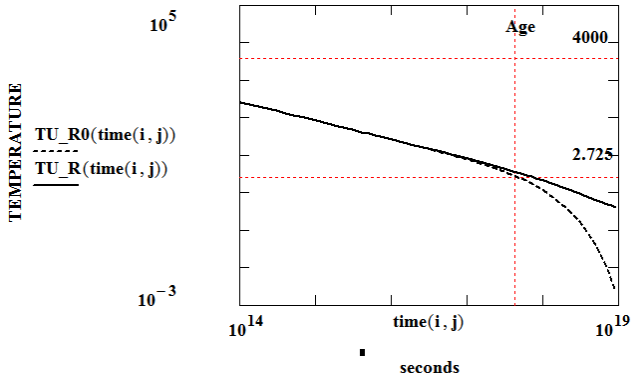

Figure 6. Radiation-observed temperature-profiles (*TU_R0* for path-altered and *TU_R* non-path-altered) of the wave-deposited radiation component; note the post-age development.

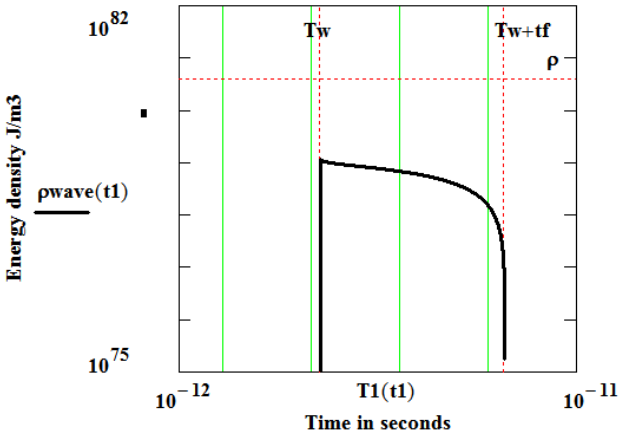

Figure 7. Shock-Wave energy-density function (J/m^3 with geometrical reduction = $1/(4\pi r^2)$ versus time on the abscissa. Time *Tw* is equal to time *tf*, the extinction time, in this graph and therefore the profile is one of the newly emerging wave.

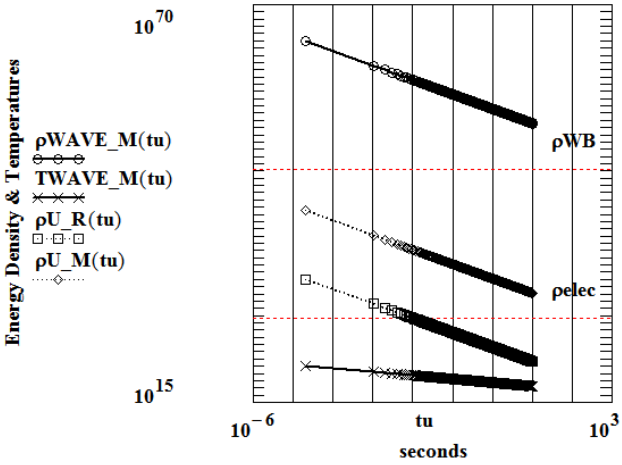

Figure 8. Matter shock-Wave (⊙) energy-density (J/m^3) and temperature functions (K) (⊠; wave) versus time on the abscissa. Deposited energy-densities (J/m^3) functions (⊡, radiation and ⧈, matter) versus time on the abscissa. The critical energy-densities, *ρWB* (W-boson) and *ρelec* (electron), already established and cited, are noted.

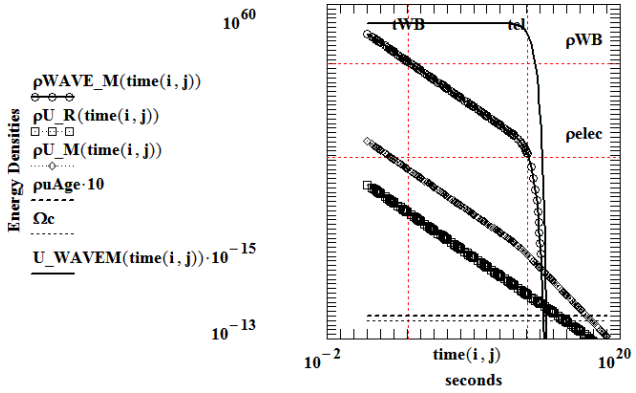

Figure 9. Matter shock-wave energy-density (J/m^3) functions (⊙; *ρWAVE_matter*) versus time on the abscissa. Deposited energy-density (J/m^3) functions (⧄ for matter and ⊡ for radiation) versus time on the abscissa. The critical boson energy-density *ρWB* and the critical electron energy-density *ρelec* in the wave are shown. The equilibrated radiation-energy-density function *ρU_rad* is depicted as (---) and the critical energy-density as (……). Also shown is the total mass-energy in the wave *U_WAVEM* (——).

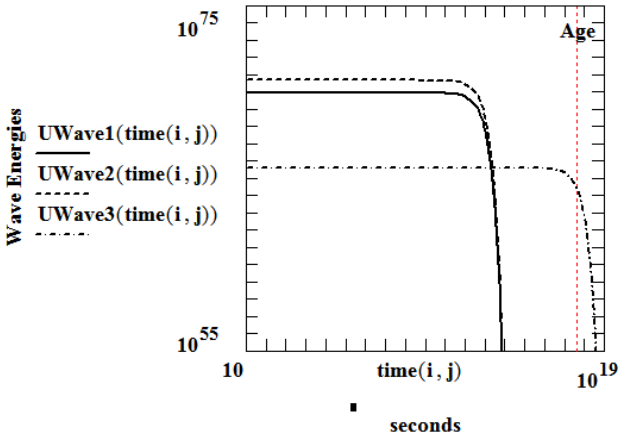

Figure 10. The depleting matter-wave-energies (*UWave* (Eq.12a) in *Joules*) (solid = 1 = *ord_matter*, dash = 2 = *dark_matter*) and the radiation-wave-energies (dadot = 3 = *rad*) vs later times in the wave's life.

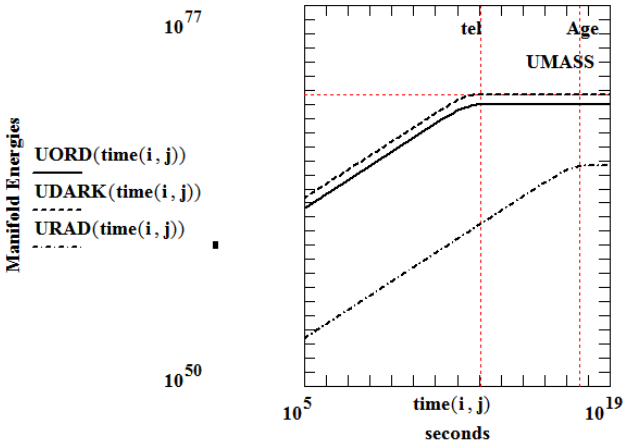

Figure 11. The accumulating manifold energies (*Joules*) (solid = *ord_matter*, dash = *dark_matter*, dadot = *radiation*) vs time in the wave's life. *time (i,j) = j(10)^{i} . UMASS = U0*.

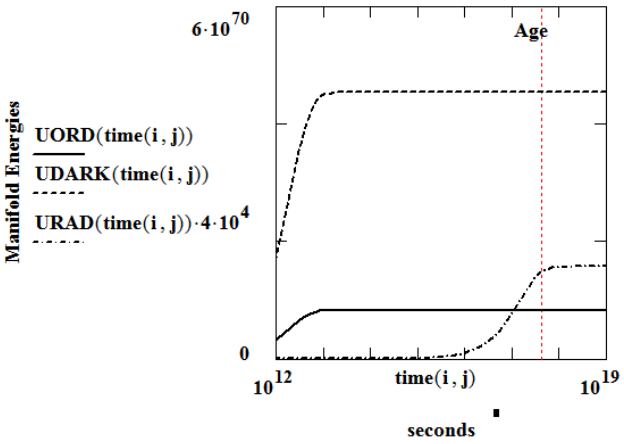

Figure 12. The accumulating manifold matter energies (*Joules*) (solid = *ord-matter*, dash = *dark-matter*) and the accumulating manifold radiation energy (*Joules*) (dadot) vs time in the wave's life.